Variable-focus terahertz lens

Benedikt Scherger,[1,2,*] Christian Jördens,[1] and Martin Koch[2]

[1]*Institut für Hochfrequenztechnik, Technische Universität Braunschweig, Schleinitzstr. 22, 38106 Braunschweig, Germany*
[2]*Fachbereich Physik, Philipps Universität Marburg, Renthof 5, 35032 Marburg, Germany*
**benedikt.scherger@physik.uni-marburg.de*

Abstract: We present a variable focus lens for the THz range. The focal length can be changed by pumping a medical white oil in and out of the lens body. Due to the optical transparency of the liquid and a similar refractive index in the visible frequency range, the THz beam path can be aligned using conventional optical light sources. This type of lens might find applications in terahertz based quality control, stand-off detection and wireless communication systems.

OCIS codes: (300.6495) Spectroscopy, terahertz; (220.3620) Lens system design; (110.6795) Terahertz imaging.

References and links

1. P. H. Siegel, "Terahertz technology," IEEE Trans. Microw. Theory Tech. **50**(3), 910–928 (2002).
2. M. Tonouchi, "Cutting-edge terahertz technology," Nat. Photonics **1**(2), 97–105 (2007).
3. D. Zimdars, J. White, G. Stuk, A. Chernovsky, G. Fichter, and S. Williamson, "Large area terahertz imaging and non-destructive evaluation applications," Insight-Non-Destruct. Test. Condition Monitor. **48**(9), 537–539 (2006).
4. C. Otani, Y. Sasaki, H. Hoshina, M. Yamashita, G. Okazaki, K. Kawase, and S. Riken-Sendai, "Development of a prototype apparatus for inspecting illicit drugs inside envelopes," in Joint 31st International Conference on Infrared Millimeter Waves and 14th International Conference on Teraherz Electronics, IRMMW-THz 2006, (2006), p. 173.
5. T. Yasui, T. Yasuda, K. Sawanaka, and T. Araki, "Terahertz paintmeter for noncontact monitoring of thickness and drying progress in paint film," Appl. Opt. **44**(32), 6849–6856 (2005).
6. C. Jördens, and M. Koch, "Detection of foreign bodies in chocolate with pulsed terahertz spectroscopy," Opt. Eng. **47**(3), 037003 (2008).
7. N. Krumbholz, T. Hochrein, N. Vieweg, T. Hasek, K. Kretschmer, M. Bastian, M. Mikulics, and M. Koch, "Monitoring polymeric compounding processes inline with THz time-domain spectroscopy," Polym. Test. **28**(1), 30–35 (2009).
8. D. Banerjee, W. von Spiegel, M. D. Thomson, S. Schabel, and H. G. Roskos, "Diagnosing water content in paper by terahertz radiation," Opt. Express **16**(12), 9060–9066 (2008).
9. P. F. Taday, "Applications of terahertz spectroscopy to pharmaceutical sciences," Philos. Transact. A Math. Phys. Eng. Sci. **362**(1815), 351–364 (2004).
10. C. Jastrow, K. Münter, R. Piesiewicz, T. Kürner, M. Koch, and T. Kleine-Ostmann, "300 GHz transmission system," Electron. Lett. **44**(3), 213–214 (2008).
11. A. Hirata, T. Kosugi, H. Takahashi, R. Yamaguchi, F. Nakajima, T. Furuta, H. Ito, H. Sugahara, Y. Sato, and T. Nagatsuma, "120-GHz-band millimeter-wave photonic wireless link for 10-Gb/s data transmission," IEEE Trans. Microw. Theory Tech. **54**(5), 1937–1944 (2006).
12. D. Turchinovich, A. Kammoun, P. Knobloch, T. Dobbertin, and M. Koch, "Flexible all-plastic mirrors for the THz range," Appl. Phys., A Mater. Sci. Process. **74**(2), 291–293 (2002).
13. W. Withayachumnankul, B. M. Fischer, and D. Abbott, "Quarter-wavelength multilayer interference filter for terahertz waves," Opt. Commun. **281**(9), 2374–2379 (2008).
14. C. Jansen, S. Wietzke, V. Astley, D. Mittleman, and M. Koch, "Mechanically flexible polymeric compound one-dimensional photonic crystals for terahertz frequencies," Appl. Phys. Lett. **96**(11), 111108 (2010).
15. R. Wilk, N. Vieweg, O. Kopschinski, and M. Koch, "Liquid crystal based electrically switchable Bragg structure for THz waves," Opt. Express **17**(9), 7377–7382 (2009).
16. S.-Z. A. Lo, and T. E. Murphy, "Nanoporous silicon multilayers for terahertz filtering," Opt. Lett. **34**(19), 2921–2923 (2009).
17. G. Gallot, S. P. Jamison, R. W. McGowan, and D. Grischkowsky, "Terahertz waveguides," J. Opt. Soc. Am. B **17**(5), 851–863 (2000).
18. K. Wang, and D. M. Mittleman, "Metal wires for terahertz wave guiding," Nature **432**(7015), 376–379 (2004).
19. M. Theuer, R. Beigang, and D. Grischkowsky, "Highly sensitive terahertz measurement of layer thickness using a two-cylinder waveguide sensor," Appl. Phys. Lett. **97**(7), 071106 (2010).

#141148 - $15.00 USD Received 14 Jan 2011; revised 11 Feb 2011; accepted 16 Feb 2011; published 23 Feb 2011

20. D. Chen, and H. Chen, "A novel low-loss Terahertz waveguide: polymer tube," Opt. Express **18**(4), 3762–3767 (2010).
21. H. Han, H. Park, M. Cho, and J. Kim, "Terahertz pulse propagation in a plastic photonic crystal fiber," Appl. Phys. Lett. **80**(15), 2634 (2002).
22. T. Ito, Y. Matsuura, M. Miyagi, H. Minamide, and H. Ito, "Flexible terahertz fiber optics with low bend-induced losses," J. Opt. Soc. Am. B **24**(5), 1230–1235 (2007).
23. K. Nielsen, H. K. Rasmussen, A. J. Adam, P. C. Planken, O. Bang, and P. U. Jepsen, "Bendable, low-loss Topas fibers for the terahertz frequency range," Opt. Express **17**(10), 8592–8601 (2009).
24. S. Atakaramians, S. Afshar V., H. Ebendorff-Heidepriem, M. Nagel, B. M. Fischer, D. Abbott, and T. M. Monro, "THz porous fibers: design, fabrication and experimental characterization," Opt. Express **17**(16), 14053–15062 (2009).
25. C. Jördens, K. Chee, I. Al-Naib, I. Pupeza, S. Peik, G. Wenke, and M. Koch, "Dielectric fibres for low-loss transmission of millimetre waves and its application in couplers and splitters," J. Infrared. Millim. Terahz. Waves **31**, 214–220 (2010).
26. R. Kersting, G. Strasser, and K. Unterrainer, "Terahertz phase modulator," Electron. Lett. **36**(13), 1156–1158 (2000).
27. T. Kleine-Ostmann, K. Pierz, G. Hein, P. Dawson, and M. Koch, "Audio signal transmission over THz communication channel using semiconductor modulator," Electron. Lett. **40**(2), 124–126 (2004).
28. H. Chen, W. Padilla, M. Cich, A. Azad, R. Averitt, and A. Taylor, "A metamaterial solid-state terahertz phase modulator," Nat. Photonics **3**(3), 148–151 (2009).
29. L. Fekete, F. Kadlec, P. Kužel, and H. Nemec, "Ultrafast opto-terahertz photonic crystal modulator," Opt. Lett. **32**(6), 680–682 (2007).
30. J. Richter, "Dielektrische Weitwinkellinsen und Speiseanordnungen für Focal Plane Array Antennen bildgebender Millimeterwellensysteme," Ph.D. thesis (Technischen Fakultät der Universität Erlangen-Nürnberg, 2006).
31. J. Lu, C. Chiu, C. Kuo, C. Lai, H. Chang, Y. Hwang, C. Pan, and C. Sun, "Terahertz scanning imaging with a subwavelength plastic fiber," Appl. Phys. Lett. **92**(8), 084102 (2008).
32. P. E. Powers, R. A. Alkuwari, J. W. Haus, K. Suizu, and H. Ito, "Terahertz generation with tandem seeded optical parametric generators," Opt. Lett. **30**(6), 640–642 (2005).
33. J. Neu, B. Krolla, O. Paul, B. Reinhard, R. Beigang, and M. Rahm, "Metamaterial-based gradient index lens with strong focusing in the THz frequency range," Opt. Express **18**(26), 27748–27757 (2010).
34. G. C. Knollman, J. L. S. Bellin, and J. L. Weaver, "Variable-focus liquid-filled hydroacoustic lens," J. Acoust. Soc. Am. **49**(1B), 253–261 (1971).
35. N. Sugiura, and S. Morita, "Variable-focus liquid-filled optical lens," Appl. Opt. **32**(22), 4181–4186 (1993).
36. A. H. Rawicz, and I. Mikhailenko, "Modeling a variable-focus liquid-filled optical lens," Appl. Opt. **35**(10), 1587–1589 (1996).
37. D.-Y. Zhang, N. Justis, V. Lien, Y. Berdichevsky, and Y.-H. Lo, "High-performance fluidic adaptive lenses," Appl. Opt. **43**(4), 783–787 (2004).
38. D. Shaw, and C.-W. Lin, "Coma compensation of O-ring driven liquid-filled lenses," Opt. Rev. **16**(2), 129–132 (2009).
39. H. Ren, and S. Wu, "Variable-focus liquid lens by changing aperture," Appl. Phys. Lett. **86**(21), 211107 (2005).
40. M. Scheller, C. Jansen, and M. Koch, "Analyzing sub-100-μm samples with transmission terahertz time domain spectroscopy," Opt. Commun. **282**(7), 1304–1306 (2009).
41. J. Birch, "The far infrared optical constants of polyethylene," Infrared Phys. **30**(2), 195–197 (1990).
42. S. Wietzke, C. Jansen, F. Rutz, D. Mittleman, and M. Koch, "Determination of additive content in polymeric compounds with terahertz time-domain spectroscopy," Polym. Test. **26**(5), 614–618 (2007).
43. C. Jördens, N. Krumbholz, T. Hasek, N. Vieweg, B. Scherger, L. Bahr, M. Mikulics, and M. Koch, "Fibre-coupled terahertz transceiver head," Electron. Lett. **44**(25), 1473–1475 (2008).

1. Introduction

During the last two decades terahertz technology has developed at a rapid pace [1,2]. Simultaneously, a large variety of potential applications for THz systems have been explored. These applications range from the stand-off detection of passengers and close-by-inspection of luggage and mail [3,4] over the monitoring of industrial production processes [5–9] to THz communications [10,11]. A mature THz technology, however, does not only require THz emitters and detectors but also passive components which can be used to guide or manipulate THz waves. The latter include frequency selective filters and reflectors [12–16] waveguides [17–20], fibers [21–24] and splitters [25] as well as modulators [26–29] and finally - as THz waves can be considered as long-waved light – also lenses. THz lenses are mostly made from polyethylene or Teflon and have therefore a fixed focal length. They are widely used in THz spectrometers [3,7], THz communication systems [10,11] and millimeter and submillimeter

#141148 - $15.00 USD Received 14 Jan 2011; revised 11 Feb 2011; accepted 16 Feb 2011; published 23 Feb 2011

wave imaging systems e.g. for stand-off detection [30]. There are also optically transparent THz lens materials like Picarin [31], Zeonex [32] or Topas which allow for an optical alignment of the THz beam path. An alternative approach is based on a metamaterial that forms a gradient index (GRIN) lens [33]. However, all of these are all solid materials so that the focal length cannot be changed during operation. In contrast to that, variable-focus lenses are known from the optical regime [34–36]. Here, we adapt the lens design for the use in quasi-optical components.

In this paper we present a variable-focus lens for the use at THz frequencies. The lens is filled with medical white oil, which is transparent at both, THz and visible frequencies. Due to a similar refractive index in both frequency ranges, such devices can be aligned using visible light.

2. Lens design

The variable-focus THz lens (VTL) consists of two polyethylene foils with a thickness of 0.15 mm. Figure 1 shows a schematic of the VTL and illustrates its operating principle. Two elastic polymer foils were clamped together with a ring shaped holder (r_s = 50 mm). The top of the holder has an opening which leaves room for a tube through which liquid can be pressed in between the two polymer layers. An increase in the liquid volume leads to an increase of the curvature of the lens surface and, hence, to a reduction in the focal length of the lens.

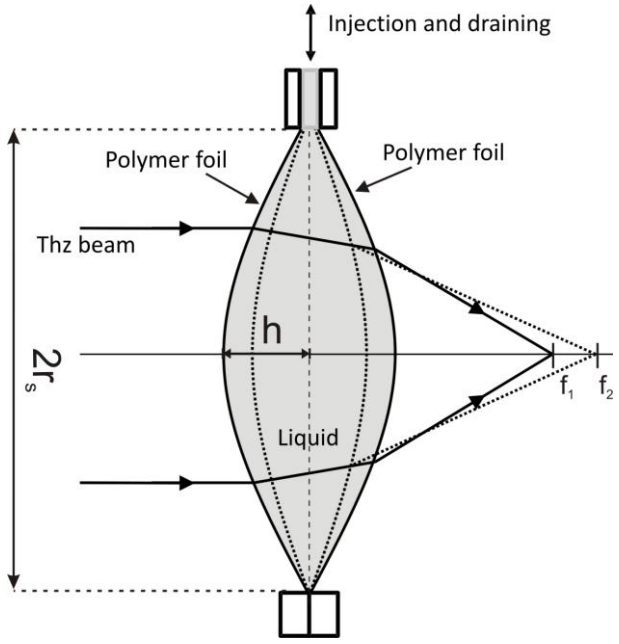

Fig. 1. Principle of the liquid filled variable focus lens. Side view of the lens for a higher and a lower filling level (solid and dashed lines) corresponding to a shorter and longer focal lengths f_1 and f_2, respectively.

If we assume that the lens surface has a spherical curvature then the radius of the sphere is:

$$r_L = \frac{r_S^2 + h^2}{2h}. \quad (1)$$

In this formula r_s is the inner radius of the circular holder and h is the height of the spherical cap (refer to Fig. 1). The volume of one of the two caps V_C of the biconvex lens is

#141148 - $15.00 USD Received 14 Jan 2011; revised 11 Feb 2011; accepted 16 Feb 2011; published 23 Feb 2011

$$V_C = \frac{\pi h}{6}(3r_S^2 + h^2). \quad (2)$$

With the well-known lens formula for the biconvex lens the volume can be associated with a focal length *f(V)*

$$\frac{1}{f(V)} = (n_L - 1)\frac{2}{r_L(V_C)}. \quad (3)$$

In this formula n_L is the refractive index of the liquid, V is the volume of the lens ($V = 2V_C$) and r_L the radius of the two caps of the biconvex lens. The radius depends on the cap volume according to Eq. (1) and Eq. (2).

For liquid-based lenses in the optical regime often polar liquids like water [37], glycerin [38] or ethanol [39] are employed. For their high absorption polar liquids cannot be used as lens materials in the THz frequency range. In our experiments we use a non polar liquid, a medical white oil (Shell Ondina 933) to fill the lens. This oil is a highly refined, non-stabilized, aromatic-free naphthenic white mineral oil, which offers a pharmaceutical purity grade. It is close to ideal for its very low THz absorption. The absorption coefficient is only 3.2cm^{-1} at 2 THz. At low THz frequencies its refractive index is nearly frequency independent with an average value of n = 1.493. Figure 2 shows the absorption coefficient (red line) and the refractive index (black line) of the oil between 0.2 and 2 THz obtained with THz time-domain spectroscopy. The foil is made of a polyethylene batch. Due to the low thickness of the foil and the accessible bandwidth of our THz-TDS system [40], we measured the refractive index of the foil with an accuracy of +/–0.02 to be n = 1.51. This value matches the data from literature very well: bulk materials consisting of low-density polyethylene (LDPE) or linear low density polyethylene (LLDPE) have a refractive index of n = 1.513 [41] or n = 1.519 [42], respectively. The refractive index of the oil (n = 1.493) and the refractive index of the polymer foil (n = 1.51) is nearly the same. Therefore, Fabry-Pérot effects arising from the oil-polymer interface are negligible. The refractive index of the oil at visible frequencies is 1.48, while the Saybolt color number is + 30. Therefore, the THz beam path can be aligned by using optical light sources.

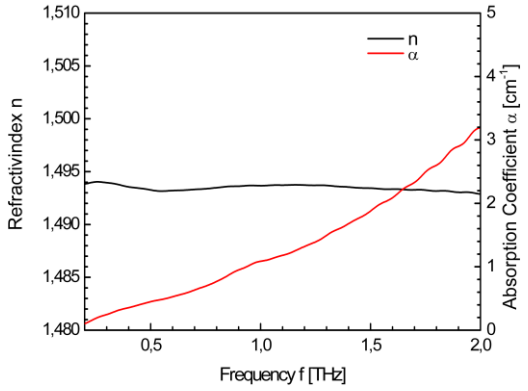

Fig. 2. Spectroscopic data of the medical white oil employed as the liquid for the lens body.

3. Results and discussion

The VTL is characterized using a fiber-coupled THz spectrometer [7] (cf. Figure 3). A lens (L1, f = 130 mm) made from high density polyethylene which is positioned after the fiber-coupled emitter antenna [43] produces a collimated THz beam with a diameter (FWHM) of 25 mm. This diameter is determined by scanning a razor blade across the THz beam. The collimated beam is then focused by the VTL onto the detector antenna. This antenna is

#141148 - $15.00 USD Received 14 Jan 2011; revised 11 Feb 2011; accepted 16 Feb 2011; published 23 Feb 2011

mounted onto a computer controlled movable stage. The profile of the focused THz beam is determined by raster scanning of the fiber-coupled receiver antenna in the x-y-plane and the x-z-plane (for axis definition cf. Figure 3). To obtain a defined "point detector" we place a small aperture of 1 mm diameter directly in front of the silicon lens of the receiver antenna. The focal plane is found via optimization of the THz amplitude by aligning the position of the VTL relative to the detector in the collimated beam (see double arrow in Fig. 3). The static lens L1, and the emitter antenna remain in a fixed position. The receiver antenna does move in x-z- and in x-y-direction when imaging the focus.

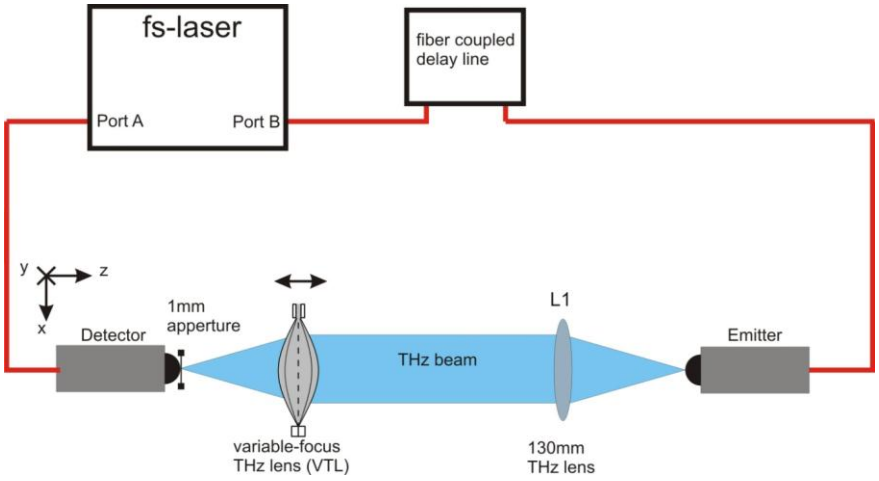

Fig. 3. Setup for scanning the profile of the THz beam after the VTL.

First, we investigate a lens with a filling volume of 155 ml corresponding to a focal length of 73 mm. To visualize the focusing properties of the lens a raster scan in the x-z plane is performed. The z-direction is the propagation direction of the THz pulse. The VTL is placed at a distance of 117 mm from the detector antenna, corresponding to z = 0 mm in Fig. 4(a). Moving the detector in positive z direction towards the VTL leads to a temporal shift of the pulse in the time domain which is compensated by the fiber coupled delay line. Figure 4(a) depicts the beam profile within a scanning range of more than 30 mm times 50 mm. We plot the intensity $I = \int |a|^2 \, dt$ of the THz time signal. In this formula a is the amplitude of the time signal which is integrated over the measured time slot in the time domain. At z = 44 mm in Fig. 4(a) (corresponding to a distance of 73 mm (i.e. the focal length) between detector and lens) a minimum diameter in x-direction is observed. Figure 4(b) shows the normalized intensity at this position. Depicted are the measured data points (dots) and a Gaussian fit (solid line) plotted over the position in the x-direction. From this graph, we obtain a minimum beam diameter (FWHM) of 2.9 mm.

#141148 - $15.00 USD Received 14 Jan 2011; revised 11 Feb 2011; accepted 16 Feb 2011; published 23 Feb 2011

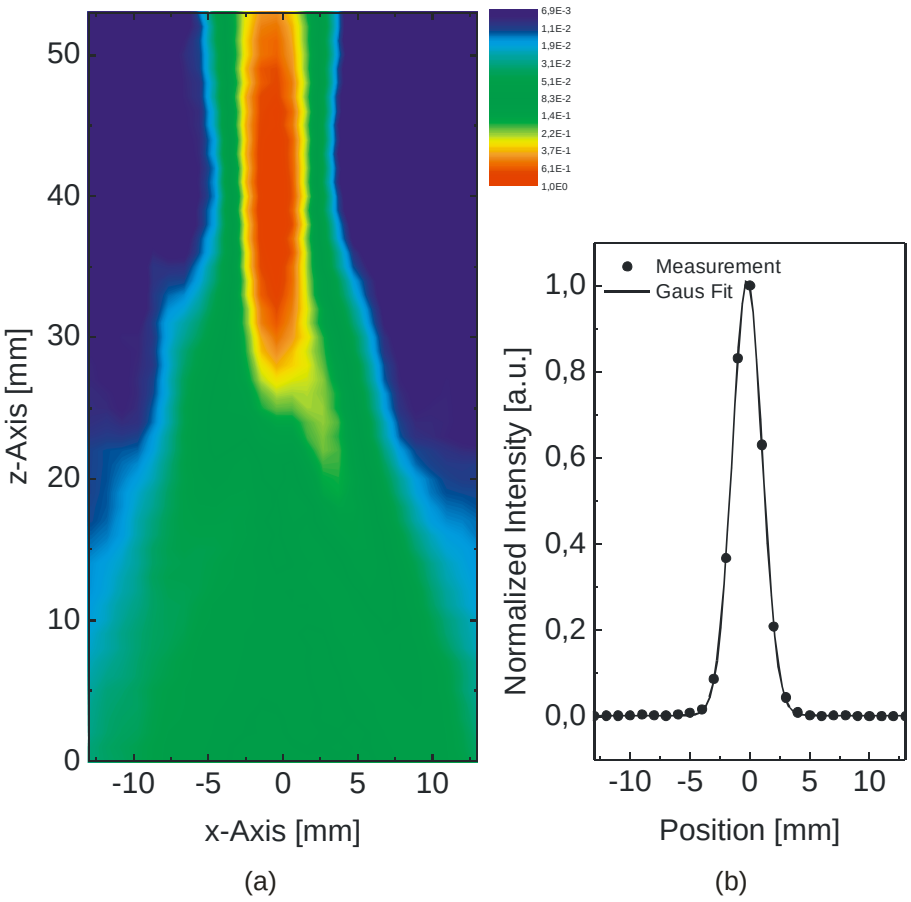

Fig. 4. (a) Beam profile in the focus region for a VTL with a focal length of 73 mm (b) Gaussian fit for the intensity along the x-axis of the THz beam at z = 44 mm.

Secondly, we compare the focusing properties of this lens (f = 73 mm, V = 155 ml) with a lens having a focal length of f = 143 mm, corresponding to a volume of V = 80 ml. Figure 5 shows the beam profiles for the longer and the shorter focal length on the left and on the right side, respectively. Figure 5(a) and 5(b) depicts the measured intensities at the corresponding focal planes in x- and y-direction. As expected the smaller focal length leads to a tighter focal spot. For both filling levels we obtain nearly round focal spots. Figure 5(c) and 5(d) displays the intensities along a line in x- (red) and y-directions (black). Again the measured data points (dots) are plotted together with the Gaussian fits (solid line). The curves for x- and y-direction coincide in both plots. The FWHM values can be read from the graph to be 4.6 mm (f = 143 mm) and 2.9 mm (f = 73 mm), respectively.

#141148 - $15.00 USD Received 14 Jan 2011; revised 11 Feb 2011; accepted 16 Feb 2011; published 23 Feb 2011

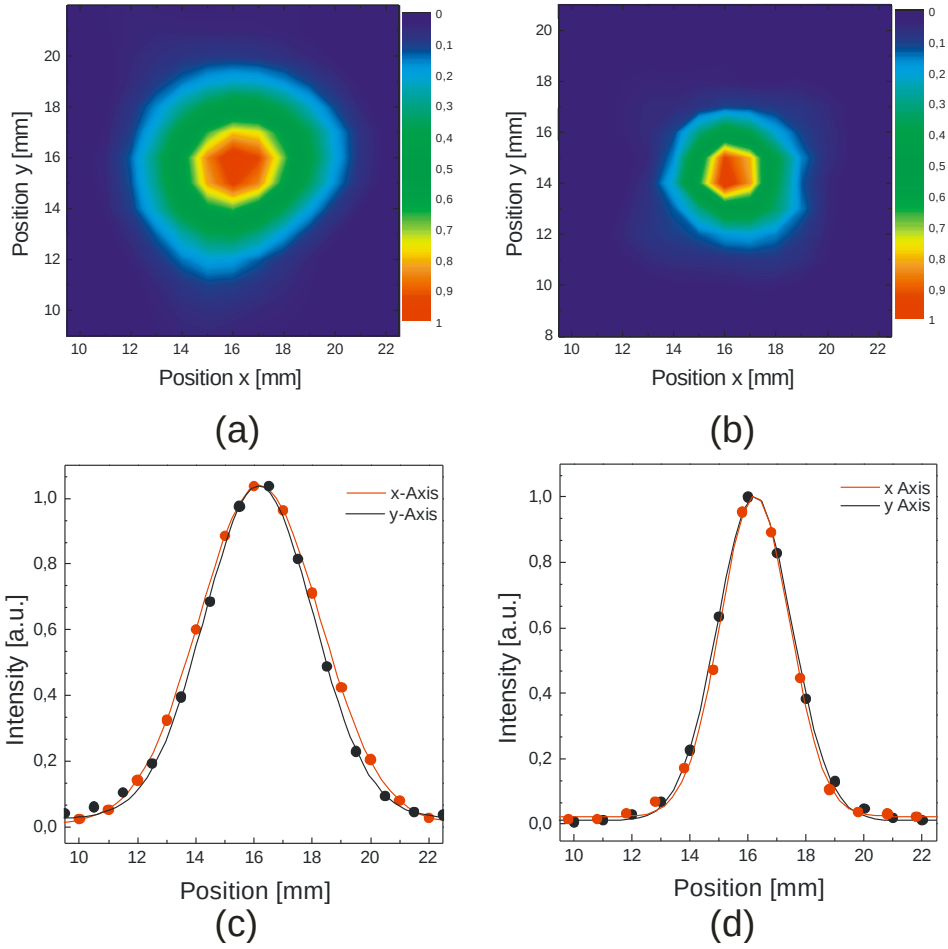

Fig. 5. (a) and (b) beam profiles for focal lengths of 143 mm and 73 mm, respectively; (c) and (d) Gaussian fits for the measured intensities along the x- and y-axis for both focal lengths.

Finally, we investigate the focal length as a function of the lens volume by multiple measurements for different filling level. The results are summarized in Fig. 6. Here, the focal length is plotted over the lens volume. Every dot corresponds to a single measurement. The theoretically expected curve according to Eqs. (1)-(3) is plotted for comparison as a solid line. We observe only slight deviations between experiment and theory. We note, some scattering of the measured results, which may arise from the dead volume in the inlet tube of the lens. Besides that, the elasticity of the foils decreases if the filling level exceeds a certain limit. Once the foil is overstretched the spherical shape of the lens body is not perfectly reproducible. For filling levels less than 60 ml we observe aberrations in the beam profile. In this case the pressure in the lens is not high enough and due to gravity the lens body deviates from the spherical shape. For filling levels above 200 ml the pressure rises to a critical level, which might cause these particular foils to rupture. Therefore, we do not investigate higher filling levels. Nonetheless the focal length of the lens can be adjusted between 50 and 240 mm.

#141148 - $15.00 USD Received 14 Jan 2011; revised 11 Feb 2011; accepted 16 Feb 2011; published 23 Feb 2011

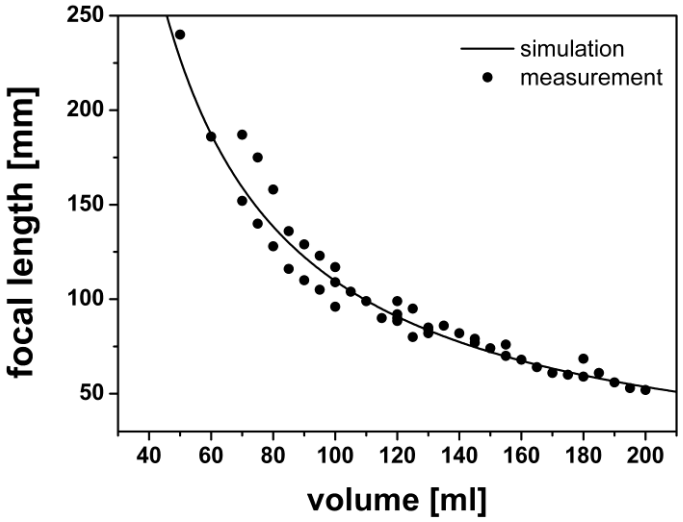

Fig. 6. Focal length of the lens for different filling levels, i.e. lens volumes. The dots represent experimental data while the solid line is the result of a calculation according to Eqs. (1) to (3).

4. Conclusion

We have experimentally demonstrated a variable-focus lens at THz frequencies. The focal length of the lens can be tuned between 50 and 240 mm. The tuning range can be further extended by the use of different, more flexible polymer foils which provide an increased elasticity. The device has a compact structure and is easy to fabricate. THz lenses with a variable focus could have great potential for imaging applications where a refocusing becomes necessary, for example for stand-off detection of moving targets. Furthermore, they could be used in terahertz communications systems when emitter or receiver (or both) move in space. In this case a refocusing of the transmitted beam will prove necessary to compensate for a different path length.

Acknowledgments

Benedikt Scherger acknowledges financial support from the Friedrich Ebert Stiftung. We thank Dirk Romeike for the mechanical construction of the VTL.

#141148 - $15.00 USD Received 14 Jan 2011; revised 11 Feb 2011; accepted 16 Feb 2011; published 23 Feb 2011